

Regulation of Vaccinia H1-related (VHR) Phosphatase Activity by NSC-87877

Sung Jin Park, Mina Song, and Sayeon Cho*

College of Pharmacy, Chung-Ang University, Seoul 156-756, Korea. *E-mail: sycho@cau.ac.kr

Received October 6, 2009, Accepted October 21, 2009

Key Words: VHR, DUSP3, NSC-87877, PTP inhibitor

Based on amino-acid sequences of catalytic domains, protein tyrosine phosphatases (PTPs) can be classified into four groups¹: class I Cys-based PTPs, class II Cys-based PTPs, class III Cys-based PTPs, and Asp-based PTPs. Each PTP has a characteristic role in a variety of cellular processes including cellular metabolism, growth, proliferation, differentiation and also has been emerged as a therapeutic target in many diseases such as diabetes, leukemia, neurodegradation, and cancer. Class I PTPs comprise dual specificity phosphatases (DUSPs) including VHR that has diverse substrate specificities both or either on phospho-Tyr, phospho-Ser, and phospho-Thr residues. Class II PTPs that dephosphorylate only pTyr are encoded by a single gene *ACP1* and related to diseases like Alzheimer's disease and asthma. Class III PTPs comprise CDC25 family proteins that regulate cell cycle by acting on Cdk. They dephosphorylate Thr-Tyr motifs of N-terminal Cdk, thus keep them from driving the cell progression.² Asp-based PTPs encoded by only four *Eya* genes recently have been listed as a new family.

VHR phosphatase, also called DUSP3, is a 20 kDa protein that might be one of the smallest known PTPs. VHR phosphatase can be elucidated by two particular characteristics in cellular physiology. First, VHR phosphatase shows more expression in the nucleus of cancer cells than that of normal cells.³ It is not due to the increase of transcription of *VHR* gene, but due to stabilization VHR phosphatase in cancer cell. Its expression was increased in cervix carcinoma and prostate cancer.⁴ Another intriguing aspect of VHR phosphatase is that it fluctuates during the phases of cell cycle. VHR phosphatase during G₁ phase is not detected due to rapid degradation. Gradually, it accumulates by means of its augmented transcription during late G₁ and S phases.⁵ The siRNA interference analyses also show that depletion of VHR phosphatase arrests cells at the G₁/S, and G₂/M phases.⁵ Highly active extracellular signal regulated kinase (ERK) is a main reason of the cell cycle arrest.⁶ Elevated VHR phosphatase expression results in cell cycle progression by dephosphorylating ERK.

Due to its elevated protein level in cancers such as cervix carcinoma and prostate cancer and involvement in cell cycle progression, VHR phosphatase has been emerged as a therapeutic target. Therefore, it is important to identify novel inhibitor of VHR phosphatase for cancer treatment. Several VHR phosphatase inhibitors including stevastelins,⁷ glucosamine- amino-ethoxy triphenyltin (GATPT),⁸ RK-682,⁹ and 4-iA¹⁰ have been identified so far. In search for more putative VHR phosphatase inhibitors, we investigated whether 8-hydroxy-7-[(6-sulfo-2-naphthyl)azo]-5-quinolinesulfonic acid (NSC-87877) has in-

hibitory effect on VHR phosphatase. NSC-87877 was originally identified as a potent SHP-2 inhibitor and showed inhibitory effect on several PTPs *in vitro*.¹¹⁻¹⁵ Active VHR phosphatase was expressed in *E. coli* as His-tagged fusion protein and purified using Ni-NTA affinity column. The inhibitory activity of NSC-87877 was then assessed against VHR phosphatase *in vitro*. NSC-87877 showed inhibitory effects on VHR phosphatase. An inhibition curve was plotted for VHR phosphatase and IC₅₀ value was calculated. The derived IC₅₀ value was 7.83 ± 0.98 μM by using the curve fitting program PRISM 3.0 (Fig. 1).

In subsequent experiments, kinetic analyses based on the Michaelis-Menten equation were performed with NSC-87877 and VHR phosphatase to provide experimental evidences for the mechanism of VHR phosphatase catalysis and for binding of the inhibitor to the active site of the phosphatase. The K_m value of VHR phosphatase for OMFP was 14.46 ± 4.05 μM (Fig. 2A). The Lineweaver-Burk plots show that the K_i was 4.09 μM (Fig. 2B). The results also show that the inhibitor acts as a competitive inhibitor of VHR phosphatase, suggesting that NSC-87877 inhibits the catalytic activity of VHR phosphatase through the binding in the catalytic site.

DUSP family can be a promising drug target for regulating the durations or quantities of activating status of mitogen-activated protein kinases (MAPKs). The regulation of phospho-

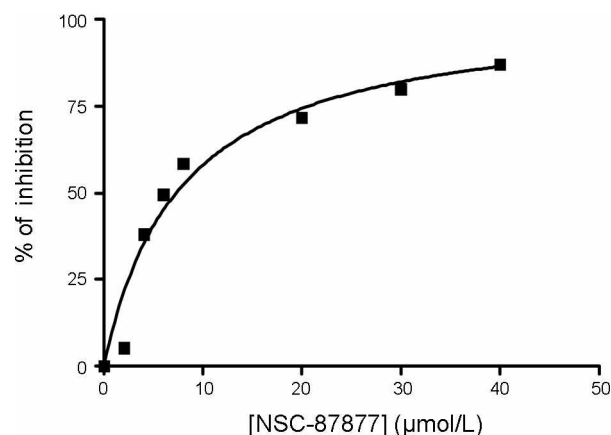


Figure 1. Inhibitory effect of NSC-87877 on VHR phosphatase. Half maximal inhibitory constant of enzyme was determined to 7.83 ± 0.98 μM. VHR phosphatase (100 nM) was incubated with various concentrations of NSC-87877 at 37 °C for 30 min. Fluorescence emission from the product was measured with a multiwell plate reader as described in Experimental section.

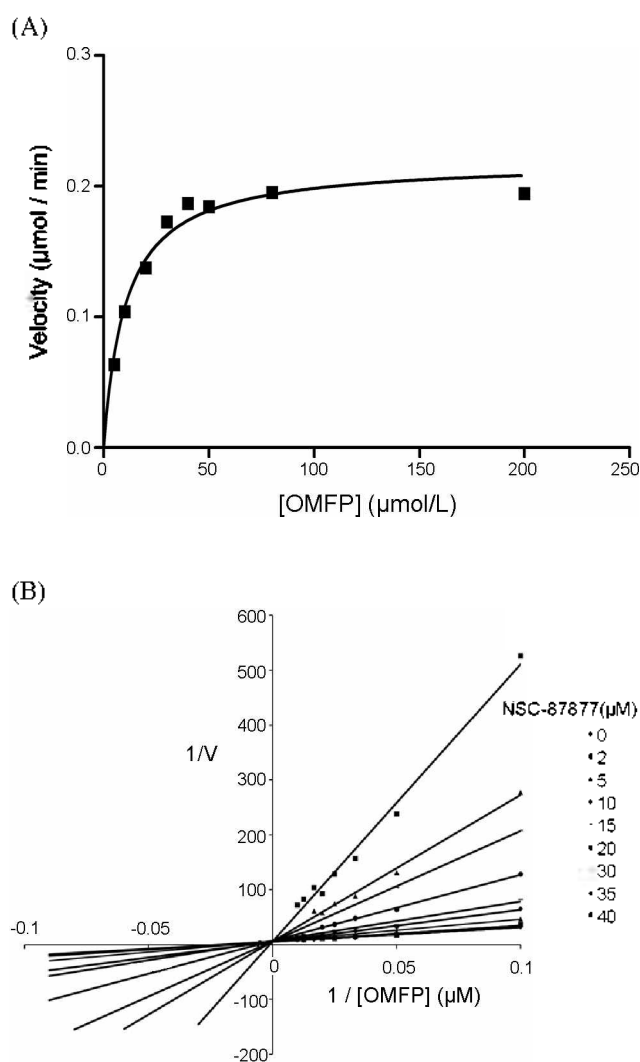


Figure 2. Kinetic analysis of VHR phosphatase inhibition by NSC-87877. (A) K_m value was determined to $14.46 \pm 4.05 \mu\text{M}$. The V_0 is plotted against OMFP substrate concentration through Michaelis-Menten enzyme analysis to calculate the $K_m = V_{max} / 2$. (B) Lineweaver-Burk plots of VHR phosphatase were generated from the reciprocal data.

proteins more depends on phosphatases than kinases. Since VHR phosphatase is a regulator of ERK,¹⁶ we examined whether the inhibitory action of NSC-87877 on VHR phosphatase influences the phosphorylation level of ERK. We performed *in vitro* phosphatase assays with recombinant phospho-ERK1 to confirm that NSC-87877 inhibits the action of VHR phosphatase on ERK1. VHR phosphatase dephosphorylates phospho-ERK and NSC-87877 inhibits phosphatase activity of VHR phosphatase toward phospho-ERK1 in a dose dependent manner (Fig. 3A). We further examined whether NSC-87877 inhibits VHR phosphatase action on endogenous ERK in cells. HEK 293 cells were transfected with FLAG-VHR expression plasmid and pretreated with various concentrations of NSC-87877 for 3 h and then stimulated with EGF to phosphorylate endogenous ERK. After 10 min of EGF treatment, cells were lysed with PTP lysis buffer. Lysates were subjected to SDS-PAGE and then immunoblotted with anti-phospho-ERK,

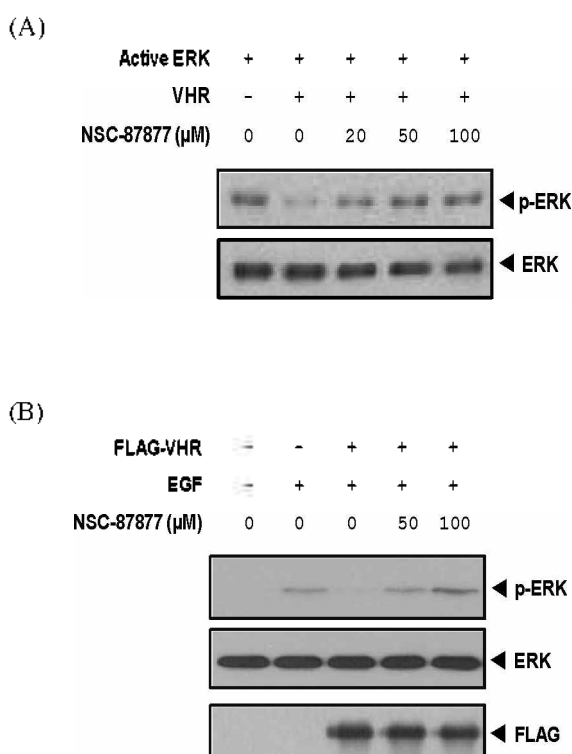


Figure 3. Inhibition of VHR phosphatase by NSC-87877 *in vitro* and *in vivo*. (A) VHR phosphatase was incubated with NSC-87877 for 10 min at 37 °C. Recombinant active ERK (20 ng) was added at 37 °C for 30 min. Dephosphorylation level of ERK was determined by western blotting analysis as described in Experiment section. (B) HEK 293 cells were transfected with FLAG-VHR expression plasmid and incubated for 48 h, and then treated with various concentrations of NSC-87877 for 3 h. After 10 min of EGF (100 ng/mL) treatment, cell lysates were separated by SDS-PAGE and analyzed by Western blotting with appropriate antibodies as described. EGF was added to stimulate endogenous ERK.

anti-ERK, and anti-FLAG antibodies, respectively (Fig. 3B). The results indicate that endogenous ERK can be effectively protected from VHR-mediated dephosphorylation by NSC-87877.

In this study, we identified NSC-87877 as a potent VHR phosphatase inhibitor and demonstrated that it could inhibit VHR phosphatase activity and therefore protect ERK kinase activity from VHR phosphatase in cells. Based on NSC-87877 inhibition of VHR phosphatase activity and high expression level of VHR phosphatase in cancer cells, NSC-87877 can be a lead compound for drug development to regulate VHR phosphatase-dependent diseases like cervix carcinoma and prostate cancer.

Experimental Section

Reagents and antibodies. Anti-ERK, anti-phospho-ERK (specific for phospho-Thr202 and phospho-Tyr204) antibodies, and active ERK protein were purchased from Cell Signaling Technology. EGF was purchased from Sigma-Aldrich (E4269). LipofectAMINE used for transfection into HEK 293 cell was purchased from Invitrogen.

Purification of the six-His-tagged VHR phosphatase. VHR expression plasmid was constructed in pET-28a (+) and transformed into BL21(DE3)-RIL *E. coli*. Recombinant VHR phosphatase was induced with 0.5 mM isopropyl- β -D-thiogalactopyranoside at 30 °C for 6 h. Cells were harvested and then lysed by sonication in 50 mM Tris-HCl (pH 8), 300 mM NaCl, 1% NP-40, and 1 mM phenylmethylsulfonyl fluoride (PMSF). The lysates were clarified at 4000 rpm for 30 min at 4 °C. The supernatant was applied by gravity flow to a column of Ni-NTA resin (PEPTRON). The resin was washed with 20 mM Tris-HCl (pH 8), 500 mM NaCl, 50 mM imidazole and eluted with 20 mM Tris-HCl (pH 8), 500 mM NaCl, 200 - 300 mM imidazole. The eluted protein was dialyzed overnight against 20 mM Tris-HCl (pH 8), 100 mM NaCl, 30% glycerol, 0.5 mM PMSF before storage at -80 °C.

In vitro phosphatase assays and kinetic analysis. The activity of VHR phosphatase was measured using the substrate 3-O-methylfluorescein phosphate (OMFP; Sigma) in a 96-well microtiter plate assay based on methods described previously.¹⁷ The NSC-87877 (Calbiochem) and OMFP were solubilized in H₂O and DMSO, respectively. All reactions were performed at a final concentration of 1% DMSO. The final incubation mixture (150 μ L) was optimized for enzyme activity and composed of 30 mM Tris-HCl (pH 7), 75 mM NaCl, 1 mM ethylenediaminetetraacetic acid (EDTA), 0.1 mM dithiothreitol (DTT), 0.33% bovine serum albumin (BSA) and 100 nM of VHR phosphatase. Reactions were initiated by addition of OMFP and incubated for 30 min at 37 °C. Fluorescence emission from product was measured with a multi-well plate reader (GENios Pro; excitation filter, 485 nm; emission filter, 535 nm). The reaction was linear over the time period of the experiment and was directly proportional to both enzyme and substrate concentration. Half-maximal inhibition constant (IC₅₀) was defined as the concentration of an inhibitor that caused a 50% decrease in the VHR phosphatase activity. Half-maximal inhibition constants and best curve fit for Lineweaver-Burk plots were determined by using the curve fitting program Prism 3.0 (GraphPad Software). All experiments were performed in triplicate and were repeated at least three times.

Dephosphorylation assays with active phosphorylated ERK. The six-His-tagged VHR phosphatase (1 μ g) was combined with active phosphorylated ERK (20 ng) in PTP assay buffer (30 mM Tris-HCl (pH 7), 75 mM NaCl, 1 mM EDTA, 0.1 mM DTT, and 0.33% BSA), and incubated for 30 min at 37 °C. To determine whether NSC-87877 inhibits VHR phosphatase effect on ERK *in vitro*, 1 μ g of VHR phosphatase was mixed with 20 ng of active phosphorylated ERK and various NSC-87877 concentrations (0, 20, 50, 100 μ M) in a 30 μ L reaction volume and incubated for 30 min at 37 °C. The samples were subjected to Western blotting analysis to examine the phosphorylation state of ERK using an anti-phospho-ERK antibody.

Western blotting analysis. Samples were run in SDS-10% polyacrylamide gels and transferred to nitrocellulose membrane. The membrane was blocked in 5% nonfat skim milk and incubated with an appropriate antibody, followed by incubation with a secondary antibody conjugated to horseradish peroxidase. The immunoreactive bands were visualized using an ECL system (Pierce, Rockford, IL).

Inhibition study. The inhibition constant (K_i) to VHR phosphatase for the inhibitor was determined by measuring the initial rates at several OMFP concentrations for each fixed concentration of the inhibitor. The data were fitted to the following equation to obtain the inhibition constant of reversible competitive inhibitors. The slopes obtained were replotted against the inhibitor concentrations. The K_i value was obtained from the slopes of these replots.⁸

$$1/V = K_m (1 + [I]/K_i) / V_{max} [S] + 1/V_{max}$$

In vivo effect of NSC-87877 on VHR phosphatase-regulated phospho-ERK. HEK 293 cells were transfected with FLAG-VHR phosphatase expression plasmid. After 48 h of transfection, cells were pretreated with NSC-87877 (0, 50, 100 μ M) for 3 h and then stimulated with EGF (100 ng/mL) for 1 h. Cells were lysed in lysis buffer containing 50 mM Tris-HCl (pH 7.5), 150 mM NaCl, 1% NP-40, 0.5% Na-deoxycholate, 1 mM EDTA, 1 mM PMSF, 1 mM Na₃VO₄, and 1 mM NaF. The samples were separated by SDS-PAGE, followed by Western blotting analysis.

Acknowledgments. This research was supported by the Chung-Ang University Research Grants in 2009.

References

- Alonso, A.; Sasin, J.; Bottini, N.; Friedberg, I.; Osterman, A.; Godzik, A.; Hunter, T.; Dixon, J.; Mustelin, T. *Cell* **2004**, *117*, 699-711.
- Honda, R.; Ohba, Y.; Nagata, A.; Okayama, H.; Yasuda, H. *FEBS Lett.* **1993**, *318*, 331-334.
- Henkens, R.; Delvenne, P.; Arafat, M.; Moutschen, M.; Zeddou, M.; Tautz, L.; Boniver, J.; Mustelin, T.; Rahmouni, S. *BMC Cancer* **2008**, *8*, 147-155.
- Arnoldussen, Y. J.; Lorenzo, P. I.; Pretorius, M. E.; Waehre, H.; Risberg, B.; Maelandsmo, G. M.; Danielsen, H. E.; Saatcioglu, F. *Cancer Res.* **2008**, *68*, 9255-9264.
- Cerignoli, F.; Rahmouni, S.; Ronai, Z.; Mustelin, T. *Cell Cycle* **2006**, *5*, 2210-2215.
- Roovers, K.; Assoian, R. K. *Bioessays* **2000**, *22*, 818-826.
- Hamaguchi, T.; Masuda, A.; Morino, T.; Osada, H. *Chem. Biol.* **1997**, *4*, 279-286.
- Shi, Z.; Tabassum, S.; Jiang, W.; Zhang, J.; Mathur, S.; Wu, J.; Shi, Y. *ChemBiochem.* **2007**, *8*, 2092-2099.
- Usui, T.; Kojima, S.; Kidokoro, S.; Ueda, K.; Osada, H.; Sodeoka, M. *Chem. Biol.* **2001**, *8*, 1209-1220.
- Ueda, K.; Usui, T.; Nakayama, H.; Ueki, M.; Takio, K.; Ubukata, M.; Osada, H. *FEBS Lett.* **2002**, *525*, 48-52.
- Chen, L.; Sung, S. S.; Yip, M. L.; Lawrence, H. R.; Ren, Y.; Guida, W. C.; Sebt, S. M.; Lawrence, N. J.; Wu, J. *Mol. Pharmacol.* **2006**, *70*, 562-570.
- Song, M.; Cho, S. *Bull. Korean Chem. Soc.* **2009**, *30*, 924-926.
- Song, M.; Cho, S. *Bull. Korean Chem. Soc.* **2009**, *30*, 1190-1192.
- Song, M.; Cho, S. *Bull. Korean Chem. Soc.* **2009**, *30*, 1858-1860.
- Song, M.; Park, S. J.; Cho, S. *Bull. Korean Chem. Soc.* **2009**, *30*, 236-238.
- Todd, J. L.; Tanner, K. G.; Denu, J. M. *J. Biol. Chem.* **1999**, *274*, 13271-13280.
- Tiemo, M. B.; Johnston, P. A.; Foster, C.; Skoko, J. J.; Shinde, S. N.; Shun, T. Y.; Lazo, J. S. *Nat. Protoc.* **2007**, *2*, 1134-1144.